Journal of Marine Science and Technology

Volume 24 | Issue 3 Article 18

ON WAVE INTERACTION WITH FLOATING STRUCTURES WITH DRAGGED MOORINGS

Po-I Chen
Department of Hydraulic and Ocean Engineering, National Cheng Kung University, Tainan, Taiwan, R.O.C,
stfanchen@gmail.com

Cheng-Tsung Chen
Department of Civil Engineering,Yancheng Institute of Technology, Yancheng City, Jiangsu province, 224051, China

Jaw-Fang Lee
Department of Hydraulic and Ocean Engineering, National Cheng Kung University, Tainan, Taiwan, R.O.C.

Recommended Citation
Chen, Po-I; Chen, Cheng-Tsung; and Lee, Jaw-Fang (2016) "ON WAVE INTERACTION WITH FLOATING STRUCTURES WITH DRAGGED MOORINGS," *Journal of Marine Science and Technology*: Vol. 24 : Iss. 3 , Article 18.
DOI: 10.6119/JMST-015-1103-1
Available at: https://jmstt.ntou.edu.tw/journal/vol24/iss3/18

ON WAVE INTERACTION WITH FLOATING STRUCTURES WITH DRAGGED MOORINGS

Acknowledgements

This work was financially supported by National Science Council of Taiwan under Grant Number NSC-96-2221-E006-332-MY3, and by Ministry of Science and Technology by Grant Number MOST 104-2221-E-006-188.

Journal of Marine Science and Technology, Vol. 24, No. 3, pp. 530-538 (2016)
DOI: 10.6119/JMST-015-1103-1

ON WAVE INTERACTION WITH FLOATING STRUCTURES WITH DRAGGED MOORINGS

Po-I Chen[1], Cheng-Tsung Chen[2], and Jaw-Fang Lee[1]

Key words: interaction, floating structure, dragged mooring, Morison equation.

ABSTRACT

This study developed an analytical solution in the frequency domain that considers the interactions among waves, floating structures, and mooring lines. The proposed solution was applied to investigate a problem involving a moored floating structure subjected to incident waves. The floating structure was considered as moving with three degrees of freedom, namely surge, heave, and roll. The mooring lines were simplified as springs, and the springs were assumed to be subjected to a Morison-type wave force. In the proposed solution, the wave field is first expressed as a problem involving a superposition of scattering and radiation waves. The wave field to be solved is expressed in terms of unknown structural motions, and wave forces acting on the floating structure and mooring springs are expressed in terms of the unknown wave fields. The solution to the coupling problem is obtained by solving the equations of motion of the floating structure with moorings. The proposed solution was simplified for evaluating cases without moorings, and its results are consistent with those of a solution in the literature. The presented solution was also used to investigate the effects of the mooring springs with added wave forces on wave fields and structural motions. The resonant amplitudes associated with the structure's motion decreased, and the peaks of resonant frequencies shifted slightly toward lower frequencies. The added mass and radiation damping coefficients versus dimensionless wave frequencies are also presented.

I. INTRODUCTION

The problems of incident waves acting on large moored floating structures include scattering and radiation problems induced by the motions of the structures; wave forces acting on small mooring lines; and interactions among incident waves, large floating structures, and small mooring structures (Sarpkaya and Isaacson, 1981). When floating structures and mooring lines are subjected to incident waves simultaneously, the surrounding wave fields engendered by the motions of the floating structures are unknown; moreover, the structural motions produced when floating structures attached to mooring lines are subjected to wave forces are unknown. Therefore, deriving a solution to the entire problem entails simultaneously solving the wave fields, motions of the floating structures, and motions of the mooring lines.

Wave forces acting on small structures can be calculated using the Morison equation because such structures do not influence incident wave forms. Solving the wave fields surrounding floating structures typically involves the superposition of scattering waves and radiation waves. The unknown amplitudes of the radiation waves are calculated by solving equations of motions of the floating structures, where the wave forces acting on the structures are calculated by combining scattering waves and radiation waves (Mei, 1983).

Calculations of wave radiation problems provide solutions to inhomogeneous boundary value problems, especially heave and roll radiation problems. Lee (1995) proposed a solution to heave radiation problems of rectangular floating structures. Chen et al. (2006) extended this solution to roll radiation problems and solved the problems of rectangular floating structures subjected to incident waves without moorings. The hydrodynamic effects of various floating structure types have been investigated. Weng and Chou (2007) studied the responses of floating dual pontoon structures subjected to incident waves. Karmakar et al. (2013) proposed using multiple floating breakwaters to reduce the wave height in a transmitted region. Finnegan and Goggins (2012) modeled the interactions of waves and floating cylinders in a numerical wave tank. Zhao and Hu (2012) numerically and experimentally studied nonlinear interactions between extreme waves and a floating body, in which highly nonlinear wave-body interactions were emphasized.

Regarding the problems of incident waves acting on moored floating structures, Ijima et al. (1972) presented a representative article. They used eigenfunction expressions for wave potentials to express the wave fields; specifically, they used series

Paper submitted 08/20/15; revised 10/27/15; accepted 11/03/15. Author for correspondence: Po-I Chen (e-mail: stfanchen@gmail.com).
[1] Department of Hydraulic and Ocean Engineering, National Cheng Kung University, Tainan, Taiwan, R.O.C.
[2] Department of Civil Engineering,Yancheng Institute of Technology, Yancheng City, Jiangsu province, 224051, China.

expressions for nonhomogeneous boundary conditions in the problem. Moreover, simple elastic springs were used to simulate the mooring lines; however, wave forces acting on the mooring lines were not considered. When examining problems of floating structures subjected to incident waves, Lee (1994) first considered wave forces acting on mooring lines. A tension-leg structure was considered, and only the surge motion of the structure was included. Lee (1994) also found that the resonant frequencies were not changed; however, the amplitudes of the structural motions were damped. Lee and Wang (2001) also studied the dynamic behaviors of tension-leg platform systems; however, they included flow-induced drag forces acting on the tethers as well as wave-induced drag forces in their study. Lee and Wang (2003) extended their research to tension-leg structure systems with twin platforms. In addition, Lee and Wang (2005) studied tension-leg-type fish cage systems subjected to incident waves. Tabeshpour et al. (2006) presented an analytical solution to the heave vibration of tension-leg platforms. Tabeshpour et al. (2013) further investigated the hydrodynamic- damped pitch motion of tension-leg platforms.

The current study investigated a two-dimensional problem of a moored floating structure subjected to incident waves. The floating structure was considered to move with three degrees of freedom (i.e., surge, heave, and roll motions), and the mooring lines were simulated using linear springs. This study also developed an analytical solution in the frequency domain, and this solution entails assessing the interactions between waves and the moored floating structure. Because wave forces acting on the mooring lines were considered, coupling effects induced by the mooring lines were also evaluated.

II. PROBLEM DESCRIPTION

The investigated problem involved a floating rectangular structure subjected to incident waves. Fig. 1 illustrates a definition sketch of the problem involving a floating structure with cross moorings. This figure shows a Cartesian coordinate system with the origin located at the still water level. The positive x-axis points to the right, and the positive z-axis points upward. In addition, h is the water depth, $2b$ is the structure's width, d is the draft, e is the protruding height above the still water level, d_0 is the diameter of the mooring line, and K_s is the stiffness of the mooring line. The incident wave propagates in the negative x direction with free surface elevation η^I. Because of the existence of the floating structure, reflected waves η_1 are generated in front of the structure, and transmitted waves η_3 are generated behind the structure. Moreover, the wave fields enforce the motions of the floating structure. The mooring lines then move along with the floating structure.

To describe the wave field, a potential function Φ is used, and is defined as follows (Dean and Dalrymple, 1991):

$$\vec{V} = -\nabla\Phi \tag{1}$$

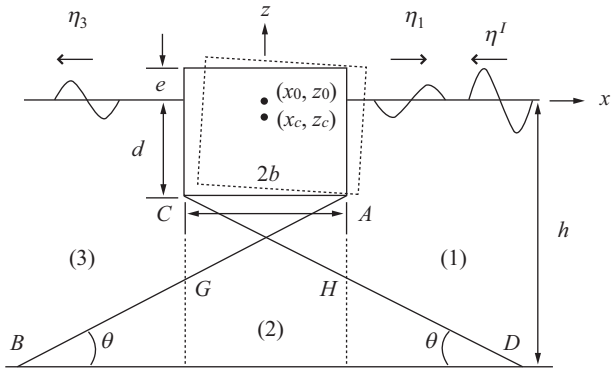

Fig. 1. Incident waves acting on a floating rectangular structure with cross moorings.

where $\vec{V}$ is the velocity and ∇ is the gradient operator. The wave fields for the aforementioned problem involve unknown disturbed wave fields in addition to incident waves. Because linear wave theory was used, the wave potentials must satisfy the Laplacian governing equation

$$\nabla^2\Phi = 0 \tag{2}$$

$$\frac{\partial\Phi}{\partial z} + \frac{1}{g}\frac{\partial^2\Phi}{\partial t^2} = 0,\ z = 0 \tag{3}$$

and the bottom boundary condition

$$\frac{\partial\Phi}{\partial z} = 0,\ z = -h \tag{4}$$

The radiation condition specifies the wave propagation direction. Moreover, a continuous normal velocity is assumed on the structural surface. The incident wave potential Φ^I can be expressed as follows:

$$\Phi^I = i\frac{A^I g}{\omega}\frac{\cosh K(z+h)}{\cosh Kh}e^{-i(Kx+\omega t)} \tag{5}$$

where A^I is the wave amplitude, K is the wave number, ω is the angular frequency, g is the gravitational constant, and $i = \sqrt{-1}$.

The equations of motion of the floating structure with three degrees of freedom and constrained by the mooring lines can be expressed as (Mei, 1983)

$$\begin{aligned}&[M]\frac{d^2}{dt^2}\begin{Bmatrix}\xi_1\\ \xi_2\\ \xi_3\end{Bmatrix} + [K]\begin{Bmatrix}\xi_1\\ \xi_2\\ \xi_3\end{Bmatrix}\\ &= \rho\int_s \Phi_t\begin{Bmatrix}n_1\\ n_2\\ n_3\end{Bmatrix}dS + \begin{Bmatrix}T_x\\ T_z\\ T_\theta\end{Bmatrix} + \int_l F^c\begin{Bmatrix}n_1\\ n_2\\ n_3\end{Bmatrix}dl\end{aligned} \tag{6}$$

and the mass matrix [*M*] and stiffness matrix [*K*] can be expressed as follows:

$$[M]=\begin{bmatrix} m & 0 & m(z_c-z_o) \\ 0 & m & -m(x_c-x_0) \\ m(z_c-z_o) & -m(x_c-x_o) & I_0 \end{bmatrix} \quad (7)$$

$$[K]=\begin{bmatrix} 0 & 0 & 0 \\ 0 & \rho g 2b & -\rho g I_x^A \\ 0 & -\rho g I_x^A & \rho g(I_{xx}^A+I_z^V)-mg(z_c-z_o) \end{bmatrix} \quad (8)$$

where m is the mass of the floating structure, $(x_{o,}\ z_o)$ is the center of the geometric center, and $(x_{c,}\ z_c)$ is the center of rotation. In addition, ξ_1, ξ_2, ξ_3 are the displacements of the floating structure in the surge, heave, and roll motions, respectively. The area moment of inertia in each direction for the rectangular floating structure can be expressed as

$$I_0 = I_x + I_z = \frac{\rho b(d+e)(d^2+2de+4e^2)}{3} \quad (9)$$

$$I_x^A = \int_{-b}^{b}(x-x_0)dx = 0 \quad (10)$$

$$I_{xx}^A = \int_{-b}^{b}(x-x_0)^2 dx = \frac{2b^2}{3} \quad (11)$$

$$I_z^V = \int_{-d}^{e}\int_{-b}^{b}(z-z_0)dxdz = be(d+e) \quad (12)$$

The first term on the right side of Eq. (6) represents the wave forces acting on the floating structure, the second term represents the restoring forces from the mooring springs, and the third term represents the wave force acting on the mooring lines. The restoring forces from the mooring springs can be expressed using displacements of the floating structure:

$$T_x = T_x^{\overline{AB}} - T_x^{\overline{CD}} \quad (13)$$

$$T_z = T_z^{\overline{AB}} + T_z^{\overline{CD}} \quad (14)$$

$$T_\theta = T_\theta^{\overline{AB}} + T_\theta^{\overline{CD}} \quad (15)$$

where

$$T_x^{\overline{AB}} = -K_{xx}^{\overline{AB}}\xi_1 - K_{xz}^{\overline{AB}}\xi_2 - K_{x\theta}^{\overline{AB}}\xi_3 \quad (16)$$

$$T_z^{\overline{AB}} = -K_{zx}^{\overline{AB}}\xi_1 - K_{zz}^{\overline{AB}}\xi_2 - K_{z\theta}^{\overline{AB}}\xi_3 \quad (17)$$

$$T_\theta^{\overline{AB}} = -K_{\theta x}^{\overline{AB}}\xi_1 - K_{\theta z}^{\overline{AB}}\xi_2 - K_{\theta\theta}^{\overline{AB}}\xi_3 \quad (18)$$

$$T_x^{\overline{CD}} = -K_{xx}^{\overline{CD}}\xi_1 - K_{xz}^{\overline{CD}}\xi_2 - K_{x\theta}^{\overline{CD}}\xi_3 \quad (19)$$

$$T_z^{\overline{CD}} = -K_{zx}^{\overline{CD}}\xi_1 - K_{zz}^{\overline{CD}}\xi_2 - K_{z\theta}^{\overline{CD}}\xi_3 \quad (20)$$

$$T_\theta^{\overline{CD}} = -K_{\theta x}^{\overline{CD}}\xi_1 - K_{\theta z}^{\overline{CD}}\xi_2 - K_{\theta\theta}^{\overline{CD}}\xi_3 \quad (21)$$

and

$$K_{xx} = K_s\cos^2,\ K_{zz} = K_s\sin^2\theta,\ K_{xz} = K_{zx} = 0 \quad (22)$$

$$K_{x\theta}^{\overline{AB}} = K_{\theta x}^{\overline{AB}} = K_{x\theta}^{\overline{CD}} = K_{\theta x}^{\overline{CD}} = \left[-\cos^2\theta\ \frac{d}{2} + \cos\theta\sin\theta(-b)\right]\rho gb \quad (23)$$

$$K_{z\theta}^{\overline{AB}} = K_{\theta z}^{\overline{AB}} = -K_{z\theta}^{\overline{CD}} = -K_{\theta z}^{\overline{CD}} = \left[-\cos\theta\sin\theta\frac{d}{2} + \sin^2\theta(-b)\right]\rho gb \quad (24)$$

$$K_{\theta\theta}^{\overline{AB}} = K_{\theta\theta}^{\overline{CD}} = \left[\cos\theta\ \frac{d}{2} - \sin\theta(-b)\right]^2\rho gb \quad (25)$$

III. ANALYTIC WAVE SOLUTIONS

The wave fields induced by the incident wave and motions of the floating structure can be expressed by the superposition of scattering waves Φ^D and radiation waves Φ^R. The radiation waves can be further decomposed, as follows, into three components corresponding to the three degrees of freedom of the structure's motion:

$$\Phi^R = \sum_{j=1}^{3} s_j \Phi^j \quad (26)$$

where s_j is the amplitude of the *j*-th degree of freedom, and Φ^j is the radiation wave potential of the *j*-th degree of freedom of the unit amplitude. The index *j* = 1, 2, 3 represents the surge, heave, and roll motions, respectively. The scattering and radiation waves can be obtained using the method of separation of variables and by dividing the problem domain into three regions (Fig. 1). According to the approach used by Chen et al. (2006), the scattering and radiation waves of a unit amplitude for the three regions can be expressed as

Region 1:

$$\Phi_1^D = \sum_{n=0}^{\infty}\frac{A_{1n}^D g\cos\left[k_n(z+h)\right]}{\omega\cos(k_n h)}\ e^{-k_n(x-\frac{b}{2})}e^{-i\omega t} \quad (27)$$

$$\Phi_1^1 = \sum_{n=0}^{\infty}A_{1n}^1\cos\left[k_n(z+h)\right]\ e^{-k_n(x-\frac{b}{2})}e^{-i\omega t} \quad (28)$$

$$\Phi_1^2 = \sum_{n=0}^{\infty} A_{1n}^2 \cos\left[k_n(z+h)\right] e^{-k_n(x-\frac{b}{2})} e^{-i\omega t} \tag{29}$$

$$\Phi_1^3 = \sum_{n=0}^{\infty} A_{1n}^3 \cos\left[k_n(z+h)\right] e^{-k_n(x-\frac{b}{2})} e^{-i\omega t} \tag{30}$$

where k_n satisfy the dispersion equation

$$\omega^2 = -gk_n \tan(k_n h) \tag{31}$$

Region 2:

$$\Phi_2^D = \frac{g}{\omega}\left\{ A_{20}^D x + B_{20}^D + \sum_{n=1}^{\infty}\left(A_{2n}^D e^{\kappa_n(x-\frac{b}{2})} + B_{2n}^D e^{-\kappa_n(x+\frac{b}{2})} \right)\cdot \cdot\cos\left[\kappa_n(z+h)\right] \right\} e^{-i\omega t} \tag{32}$$

$$\Phi_2^1 = \left\{ A_{20}^1 x + B_{20}^1 + \sum_{n=1}^{\infty}\left(A_{2n}^1 e^{\kappa_n(x-\frac{b}{2})} + B_{2n}^1 e^{-\kappa_n(x+\frac{b}{2})} \right)\cdot \cdot\cos\left[\kappa_n(z+h)\right] \right\} e^{-i\omega t} \tag{33}$$

$$\Phi_2^2 = (\sum_{n=1}^{\infty} \tilde{A}_{2n}^2 \sin\left[\lambda_n(x-\frac{b}{2})\right]\cosh\left[\lambda_n(z+h)\right] + A_{20}^2 x + B_{20}^2 + \sum_{n=1}^{\infty}\left(A_{2n}^2 e^{\kappa_n(x+\frac{b}{2})} + B_{2n}^2 e^{-\kappa_n(x-\frac{b}{2})} \right)\cos\left[\kappa_n(z+h)\right])e^{-i\omega t} \tag{34}$$

$$\Phi_2^3 = (\sum_{n=1}^{\infty} \tilde{A}_{2n}^3 \sin\left[\lambda_n(x-\frac{b}{2})\right]\cosh\left[\lambda_n(z+h)\right] + A_{20}^3 x + B_{20}^3 + \sum_{n=1}^{\infty}\left(A_{2n}^3 e^{\kappa_n(x+\frac{b}{2})} + B_{2n}^3 e^{-\kappa_n(x-\frac{b}{2})} \right)\cos\left[\kappa_n(z+h)\right])e^{-i\omega t} \tag{35}$$

where

$$\tilde{A}_{2n}^2 = \frac{i\omega^2 s_2\left(\cos 2\lambda_n b - 1\right)}{g\lambda_n^2 \sinh\lambda_n\left(h-d\right)} \quad , \; n = 1, 2, 3, \ldots \tag{36}$$

$$\tilde{A}_{2n}^3 = \frac{i\omega^2 s_3\left(\cos 2\lambda_n b + 1\right)}{g\lambda_n^2 \sinh\lambda_n\left(h-d\right)} \quad , \; n = 1, 2, 3, \ldots \tag{37}$$

$$\lambda_n = \frac{n\pi}{2b}, \; n = 1, 2, 3, \ldots \tag{38}$$

$$\kappa_n = \frac{n\pi}{h-d}, \; n = 1, 2, 3, \ldots \tag{39}$$

Region 3：

$$\Phi_3^D = \sum_{n=0}^{\infty} \frac{A_{3n}^D g\cos\left[k_n(z+h)\right]}{\omega\cos(k_n h)} e^{k_n(x+\frac{b}{2})} e^{-i\omega t} \tag{40}$$

$$\Phi_{3n}^1 = \sum_{n=0}^{\infty} A_{3n}^1 \cos\left[k_n(z+h)\right] e^{k_n(x+\frac{b}{2})} e^{-i\omega t} \tag{41}$$

$$\Phi_{3n}^2 = \sum_{n=0}^{\infty} A_{3n}^2 \cos\left[k_n(z+h)\right] e^{k_n(x+\frac{b}{2})} e^{-i\omega t} \tag{42}$$

$$\Phi_{3n}^3 = \sum_{n=0}^{\infty} A_{3n}^3 \cos\left[k_n(z+h)\right] e^{k_n(x+\frac{b}{2})} e^{-i\omega t} \tag{43}$$

The first subscripts of the wave potentials in Eqs. (27)-(43) represent the region associated with the evaluated wave potential. The undetermined coefficients in Eqs. (27)-(43) can be determined using the matching conditions between neighboring regions at boundaries $x = +b$ and $x = -b$.

The wave forces acting on the mooring lines can be calculated using the Morison equation. A linearized form of this equation can be written as follows (Sollitt and Cross, 1972):

$$F^C = \rho R_d D(U - \dot{\xi}) + \rho C_m \forall\left(\frac{\partial U}{\partial t} - \ddot{\xi}\right) \tag{44}$$

where C_m is the inertia coefficient, ρ is the fluid density; D is the projection area per unit length; $\forall$ is the volume per unit length; U and $\partial U/\partial t$ are the flow velocity and acceleration normal to the mooring lines, respectively, and $\dot{\xi}$ and $\ddot{\xi}$ are the velocity and acceleration of the mooring lines, respectively.

The linear drag coefficient R_d is defined as

$$R_d = \frac{\int_0^T \int_{-h}^{-d}\left[0.5\rho D C_d \left|U - \dot{\xi}\right|(U - \dot{\xi})\right](U - \dot{\xi})dzdt}{\int_0^T \int_{-h}^{-d}\left[\rho D C_d (U - \dot{\xi})\right](U - \dot{\xi})dzdt} \tag{45}$$

where C_d is the drag coefficient.

The wave forces acting on mooring lines $\overline{AB}$ and $\overline{CD}$ can be expressed as

$$F_{\overline{AB}}^c = \int_{-h}^{-\frac{2b+3d}{3}} F_{\overline{GB}}^c \, dz + \int_{-\frac{2b+3d}{3}}^{-d} F_{\overline{AG}}^c \, \mathrm{dz} \tag{46}$$

$$F_{\overline{CD}}^c = \int_{-h}^{-\frac{2b+3d}{3}} F_{\overline{HD}}^c \, dz + \int_{-\frac{2b+3d}{3}}^{-d} F_{\overline{CH}}^c \, \mathrm{dz} \tag{47}$$

where $F_{\overline{GB}}^c$ and $F_{\overline{AG}}^c$ are the wave forces acting on mooring line $\overline{AB}$ and are calculated according to the wave potentials in

regions III and II, respectively. Moreover, $F^c_{\overline{HD}}$ and $F^c_{\overline{CH}}$ are the wave forces acting on mooring line $\overline{CD}$ and are calculated according to the wave potentials in regions I and II, respectively.

$$F^c_{\overline{GB}} = \left[R_d \rho\omega D U_3 + \frac{1}{4}\rho\pi D^2 C_m \dot{U}_3 \right] + \left[\frac{1}{4}\rho\pi D^2 \ddot{\xi}_{\overline{GB}}(1+C_m) - R_d \rho\omega D \dot{\xi}_{\overline{GB}} \right] \quad (48)$$

$$F^c_{\overline{AG}} = \left[R_d \rho\omega D U_2 + \frac{1}{4}\rho\pi D^2 C_m \dot{U}_2 \right] + \left[\frac{1}{4}\rho\pi D^2 \ddot{\xi}_{\overline{AG}}(1+C_m) - R_d \rho\omega D \dot{\xi}_{\overline{AG}} \right] \quad (49)$$

$$F^c_{\overline{HD}} = \left[R_d \rho\omega D U_1 + \frac{1}{4}\rho\pi D^2 C_m \dot{U}_1 \right] + \left[\frac{1}{4}\rho\pi D^2 \ddot{\xi}_{\overline{HD}}(1+C_m) - R_d \rho\omega D \dot{\xi}_{\overline{HD}} \right] \quad (50)$$

$$F^c_{\overline{CH}} = \left[R_d \rho\omega D U_2 + \frac{1}{4}\rho\pi D^2 C_m \dot{U}_2 \right] + \left[\frac{1}{4}\rho\pi D^2 \ddot{\xi}_{\overline{CH}}(1+C_m) - R_d \rho\omega D \dot{\xi}_{\overline{CH}} \right] \quad (51)$$

The flow velocities in Eqs. (48)-(51) can be calculated using the expressions derived for the scattering and radiation waves [i.e., Eqs. (27)-(43)]:

$$U_1 = -(\Phi^I_{,x} + \Phi^D_{1,x} + s_1\Phi^1_{1,x} + s_2\Phi^2_{1,x} + s_3\Phi^3_{1,x})\cos\theta - (\Phi^I_{,z} + \Phi^D_{1,z} + s_1\Phi^1_{1,z} + s_2\Phi^2_{1,z} + s_3\Phi^3_{1,z})\sin\theta \quad (52)$$

$$U_2 = -(\Phi^I_{,x} + \Phi^D_{2,x} + s_1\Phi^1_{2,x} + s_2\Phi^2_{2,x} + s_3\Phi^3_{2,x})\cos\theta - (\Phi^I_{,z} + \Phi^D_{1,z} + s_1\Phi^1_{2,z} + s_2\Phi^2_{2,z} + s_3\Phi^3_{2,z})\sin\theta \quad (53)$$

$$U_3 = -(\Phi^I_{,x} + \Phi^D_{3,x} + s_1\Phi^1_{3,x} + s_2\Phi^2_{3,x} + s_3\Phi^3_{3,x})\cos\theta - (\Phi^I_{,z} + \Phi^D_{3,z} + s_1\Phi^1_{3,z} + s_2\Phi^2_{3,z} + s_3\Phi^3_{3,z})\sin\theta \quad (54)$$

where the subscript commas indicate differentiation. The notation U_j represents the flow velocity located in the j-th region. The displacements of mooring lines AB and CD can be readily calculated according to geometrical deployments of the mooring lines.

$$\xi_{\overline{AB}} = \xi_{\overline{CD}} = \left(\frac{h+z}{h-d}\right)(S_1 + S_3\frac{d}{2})e^{-i\omega t}\hat{i} + \left(\frac{3h-3d-x-b}{3h-3d}\right)(S_2 + S_3 b)e^{-i\omega t}\hat{j} \quad (55)$$

After the substitutions of the wave potentials [Eqs. (27)-(43)], mooring forces [Eqs. (13)-(25)], and wave forces on the mooring lines [Eqs. (46)-(51)] and the consideration of a periodic function in time, the structure's equations of motion [Eq. (6)] can be rewritten as follows:

$$(-\omega^2[M] + [K] + i\omega\rho[F^{ra}] + [F^{wa}])\{s\} = -i\omega\rho\{F^D\} + \{F^{wD}\} \quad (56)$$

where $[F^{ra}]$ and $[F^{wa}]$ are coefficient matrices derived on the basis of wave forces, which are calculated according to the unit amplitude of the radiation waves, acting on the floating structure and mooring lines, respectively. Furthermore, $\{F^{wD}\}$ and $\{F^D\}$ are column matrices obtained on the basis of the wave forces, which are calculated according to the scattering waves (including incident waves), acting on the floating structure and mooring lines, respectively. The term $\{s\}$ in Eq. (56) is a column vector equivalent to the transpose of $\{s_1\ s_2\ s_3\}$. In Eq. (56), the coefficient matrix $[F^{ra}]$ can be rearranged further. The imaginary part is used to define the added mass coeffcients.

$$[\mu] = \begin{bmatrix} \Im\left(F^{ra}_{11}\right)/\omega^2 m & 0 & \Im\left(F^{ra}_{13}\right)/\omega^2 m \\ 0 & \Im\left(F^{ra}_{22}\right)/\omega^2 m & 0 \\ \Im\left(F^{ra}_{31}\right)/\omega^2 I_0 & 0 & \Im\left(F^{ra}_{33}\right)/\omega^2 I_0 \end{bmatrix} \quad (57)$$

The corresponding real part is used to define the radiation damping.

$$[\lambda] = \begin{bmatrix} \Re\left(F^{ra}_{11}\right)/\omega^2 m & 0 & \Re\left(F^{ra}_{13}\right)/\omega^2 m \\ 0 & \Re\left(F^{ra}_{22}\right)/\omega^2 m & 0 \\ \Re\left(F^{ra}_{31}\right)/\omega^2 I_0 & 0 & \Re\left(F^{ra}_{33}\right)/\omega^2 I_0 \end{bmatrix} \quad (58)$$

Eq. (56) can be solved for the three degrees of freedom of the structure's motion. The radiation waves can then be calculated using Eq. (26). Once the wave potentials are determined, the surface elevations can be obtained by applying Bernoulli's equation. Subsequently, the reflected and transmitted surface elevations can be used to calculate the wave amplitudes, followed by the reflecting and transmitting coefficients K_r and K_t.

IV. RESULTS AND DISCUSSION

To demonstrate the accuracy of the proposed solution, this study assessed the problem of a floating rectangular structure with spring moorings evaluated by Ijima et al. (1972). The proposed solution was simplified for cases involving mooring lines without wave loadings. Fig. 2 shows comparisons of reflection coefficients between the proposed analytical solution and that presented by Ijima et al. (1972). The calculation con-

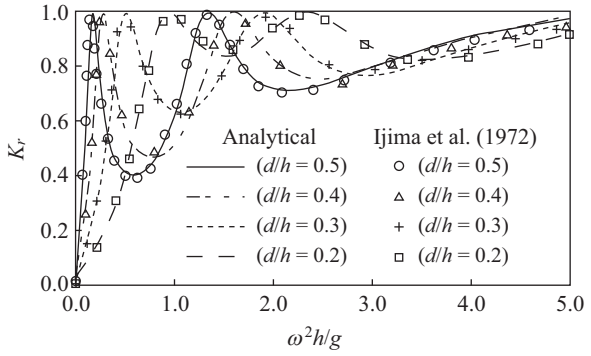

Fig. 2. Comparisons of the reflection coefficients between the proposed analytical solution and that of Ijima et al. (1972) for various drafts.

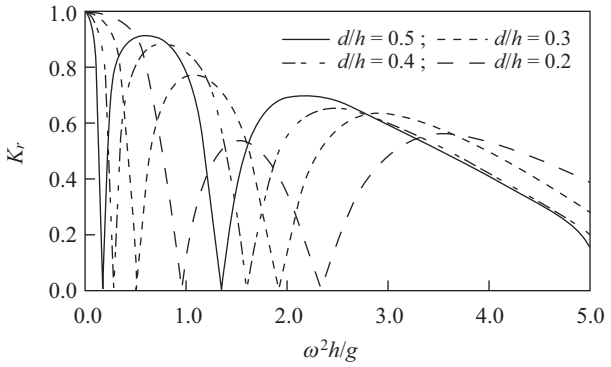

Fig. 3. Effects of structure submergence on transmission coefficients.

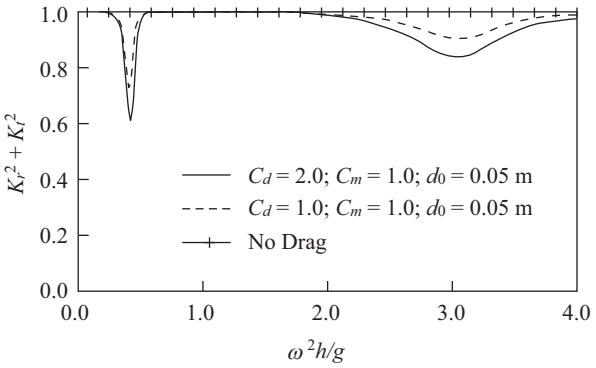

Fig. 4. Effects of friction coefficients on the total energy.

ditions are outlined as follows: water depth = 10 m; structure width = 10 m; structure material density = 0.8; spring stiffness $K = \rho_w g b$; and floating structure submergence d/h = 0.2, 0.3, 0.4, and 0.5. The comparisons in Fig. 2 indicate that without a mooring drag consideration, the results of the proposed solution effectively reflect the simulation results. Fig. 3 illustrates transmission coefficients corresponding to the results shown in Fig. 2. The reflection and transmission coefficients can also be used to examine the conservation of energy for the problem system involving no energy dissipation. Fig. 3 also indicates that shorter incident waves result in smaller transmitted waves.

To investigate the effects of mooring drags on the problem,

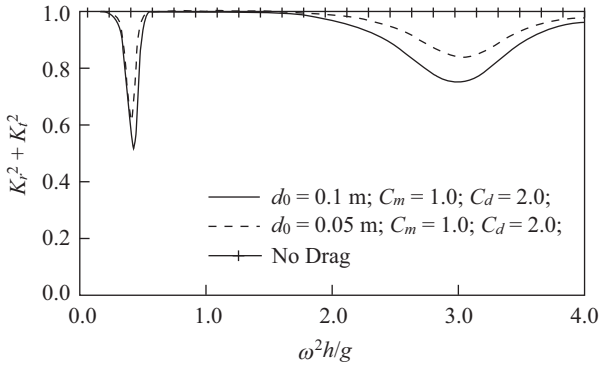

Fig. 5. Effects of mooring line diameters on the total energy.

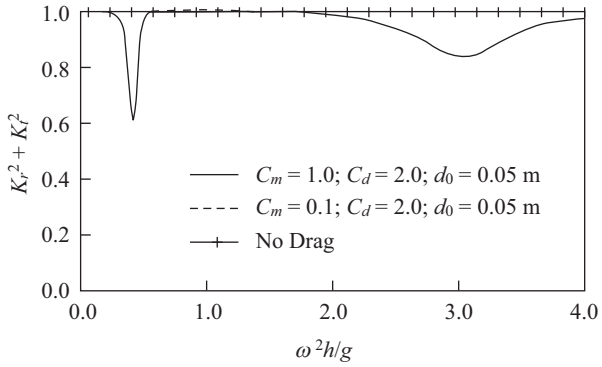

Fig. 6. Effects of inertia coefficients on the total energy.

the parameters of the friction coefficients, added mass coefficients, and mooring line diameters were considered. The calculation conditions are outlined as follows: water depth = 10 m, floating structure width = 2 m, submergence depth d = 2 m, mooring line spring stiffness $K = \rho_w g b$, mooring line diameter = 0.05 m, inertia coefficient = 1.0, and friction coefficients = 1.0 and 2.0. Fig. 4 shows the effects of various friction coefficients on the total energy expressed in terms of reflection and transmission coefficients, indicating that an increased friction drag induces discernible energy damping in the vicinity of resonant frequencies and that a higher friction drag results in a higher energy damping magnitude. Fig. 5 illustrates the effects of various mooring line diameters on the total energy, signifying that a larger mooring line diameter engenders a higher friction drag on the mooring lines, consequently inducing higher energy damping. This figure also indicates that heavier mooring lines cause the resonant frequency to shift slightly toward lower values. Fig. 6 shows the effects of diverse inertia coefficients on the total energy of the wave field. In this computation, the friction coefficient was set to 2.0 and the mooring line diameter was set to 0.05 m. The results revealed that the inertia coefficients did not alter the energy magnitude of the wave-structure system and that the friction coefficient induced energy damping in the vicinity of the resonant frequency.

The effects of friction coefficients on the motions of the floating structure are presented subsequently. Fig. 7 shows the floating structure's surge motions corresponding to various

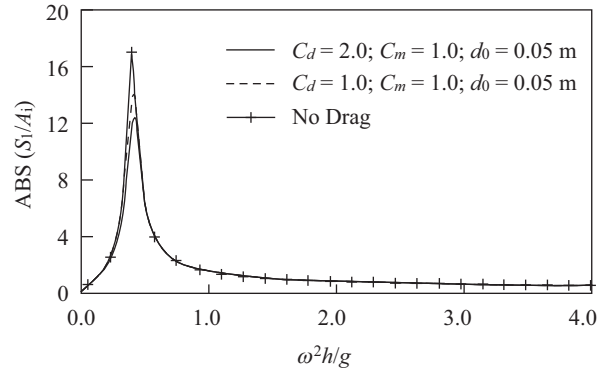

Fig. 7. Effects of friction coefficients on the dimensionless surge amplitudes of the floating structure.

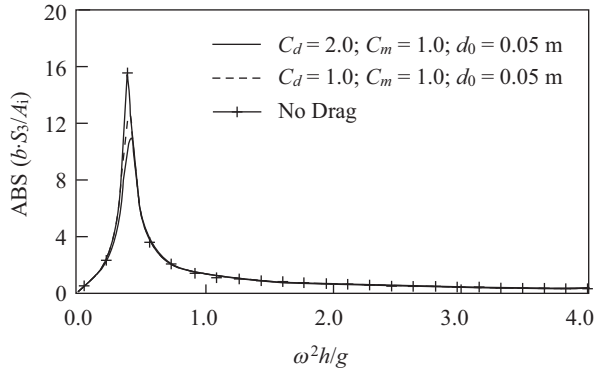

Fig. 9. Effects of friction coefficients on the dimensionless roll amplitudes of the floating structure.

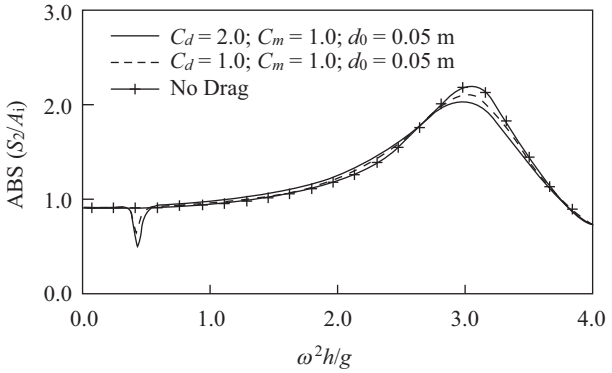

Fig. 8. Effects of friction coefficients on the dimensionless heave amplitudes of the floating structure.

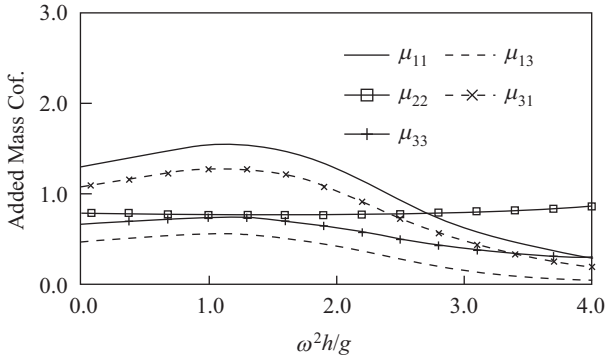

Fig. 10. Added mass coefficient versus dimensionless wave frequencies for each degree of freedom.

friction coefficients without drag; this figure shows a plot of dimensionless surge amplitudes versus dimensionless wave frequencies. The inertia coefficient was set to 1.0 and the mooring line diameter was set to 0.05 m. The results indicated that increasing the friction coefficient changed the response curve only at the resonant peak. In addition, when the mooring drag was considered, the friction coefficient did not induce a change in the structural motion response curve, except in the vicinity of the resonant peak.

Fig. 8 illustrates the effects of various friction coefficients on the floating structure's heave motion, showing a plot of dimensionless heave amplitudes versus dimensionless wave frequencies. The results revealed that when the friction coefficient was increased, the response curves tended to demonstrate a decreasing trend in the vicinity of resonant peaks, whereas they remained unchanged elsewhere. For the evaluated conditions, the structure's motion in the heave direction was smaller than the surge motion shown in Fig. 7. Fig. 9 shows the effects of different friction coefficients on the floating structure's roll motion. Similar to the surge and heave motion results (Figs. 7 and 8, respectively), the response curves of the floating structure decreased in the vicinity of resonant peaks and remained constant elsewhere. On the basis of the response curves corresponding to the three degrees of freedom of the floating structure, one can conclude that when the mooring drag is considered, the structure's motions are damped only in the vicinity of resonant peaks, with limited changes occurring elsewhere. Furthermore, when the inertia coefficients are included in the Morison equation, the resonant frequency tends to shift slightly toward lower values.

The added mass and radiation damping coefficients for the moored floating structure was calculated using the presented analytical solution. Fig. 10 shows plots of the added mass coefficients versus dimensionless wave frequencies for the structure's motion along each degree of freedom; the added mass coefficients correspond to the surge (μ_{11}), heave (μ_{22}), and roll (μ_{33}) motions in addition to the effect of roll motion on surge motion (μ_{13}) and the effect of surge motion on roll motion (μ_{31}). The results revealed that the added mass coefficients were monotonic functions of dimensionless depth. The added mass coefficients for the surge and roll motions increased monotonically at shallower waters and peaked at $\omega^2 h/g$ = 1.2, and they decreased monotonically for deeper waters. By contrast, for the heave motion, the variation of the added mass coefficient was within a narrow range. The minimum value of the coefficient was $\omega^2 h/g$ = 1.5, and it subsequently increased monotonically with respect to the dimensionless water fre-

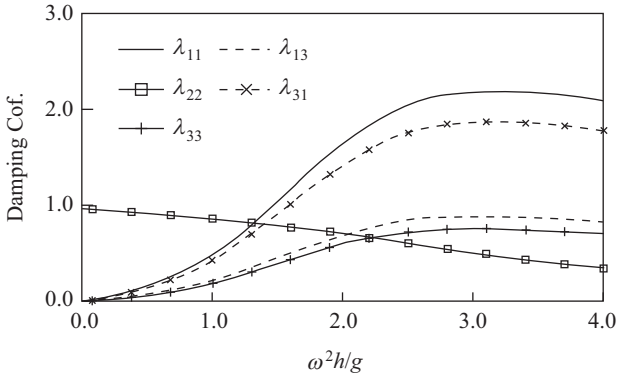

Fig. 11. Radiation damping coefficients versus dimensionless wave frequencies for each degree of freedom.

quency. The increase in the added mass coefficients indicated that the floating structure had a high virtual mass, thereby raising the difficulty of the structure in responding to external wave forces. Therefore, for the heave motion, the floating structure encountered greater difficulty moving in deeper waters; nevertheless, for the surge and roll motions, the floating structure more easily responded to wave forces. Fig. 10 also shows the added mass coefficients representing the effect of roll motion on surge motion (μ_{13}), and vice versa (μ_{31}). The added mass coefficient μ_{31} is higher than μ_{13}, indicating that the surge motion exerts higher effects on the roll motion (instead of the other way around) for the entire range of water depths.

The radiation damping of the ocean structure represents scattered and/or radiated outgoing waves, which transmit wave energy from the floating structure, and is expressed as energy damping of the structure system. Higher radiation damping indicates a higher amount of waves that propagate away from the structure system. Fig. 11 shows plots of radiation damping coefficients versus dimensionless wave frequencies for components of the damping matrix of the floating structure. The radiation damping coefficient for the heave motion decreased monotonically with respect to the dimensionless wave frequency, implying that for deeper depth incident waves, the radiated waves are smaller. However, for the surge and roll motions, the radiation damping coefficients increased with the water depth and peaked at $\omega^2 h/g = 3.18$. Similar to the results shown in Fig. 10. Fig. 11 also shows the radiation damping coefficients representing the effect of the roll motion on the surge motion (λ_{13}), and vice versa (λ_{31}). The radiation damping coefficient λ_{31} is higher than λ_{13}, indicating that the surge motion has a higher effect on the roll motion (instead of the other way around) for the entire range of water depths.

V. CONCLUSIONS

This study developed an analytical solution to a problem involving the interaction of wave forces with a moored floating structure. In this solution, wave forces acting on mooring lines are considered. The proposed solution was simplified to evaluate cases without mooring drags, and the results it yielded were highly consistent with those reported by Ijima et al. (1972). When wave forces acting on the mooring lines were included, the examination of the energy conservation of the wave system revealed that increasing the friction drag induced discernible energy damping in the vicinity of the resonant frequencies and that a higher friction drag resulted in a higher energy damping magnitude. However, the inertia coefficients did not alter the energy magnitude of the wave system. The effects of various friction coefficient values on the motions of the floating structure were also observed, and the results indicated that when the friction coefficient was high, the response curves dropped only at the resonant peak and remained constant elsewhere. The analytical solution was also used to determine the added mass and radiation damping coefficients for the moored floating structure.

ACKNOWLEDGEMENTS

This work was financially supported by National Science Council of Taiwan under Grant Number NSC-96-2221-E-006-332-MY3, and by Ministry of Science and Technology by Grant Number MOST 104-2221-E-006-188.

REFERENCES

Chen, P. I., J. F. Lee and W. S. Horng (2006). Analytic solution of waves acting on floating structures. Journal of Coastal and Ocean Engineering 6(2), 63-80.

Dean, R. G. and R. A. Dalrymple (1991). Water mechanics for Scientists and Engineers. World Scientific.

Finnegan,W. and J. Jamie Goggins (2012). Numerical simulation of linear water waves and wave-structure interaction. Ocean Engineering 43, 23-31.

Ijima, T., Y. Tabuchi and Y. Yumura (1972). Scattering of surface waves and the motions of a rectangular body by waves in finite water depth. Proceedings of Japan Society of Civil Engineers 202, 33-48.

Karmakar, D., J. Bhattacharjee and C. G. Soares (2013). Scattering of gravity waves by multiple surface-piercing floating membrane. Applied Ocean Research 39, 40-52.

Lee, C. P. (1994). Dragged Surge Motion of A Tension Leg Structure. Ocean Engineering 21(3), 311-328.

Lee, H. H. and W. S. Wang (2001). Analytical Solution on the Dragged Surge Vibration of TLPs with Wave Large Body and Small Body Multi-interactions. Journal of Sound and Vibration 248(3), 533-556.

Lee, H. H. and W. S. Wang (2003). On the Dragged Surge Vibration of a Twin TLP System with Multi-Interactions of Wave and Structures. Journal of Sound and Vibration 263(4), 743-774.

Lee, H. H. and W. S. Wang (2005). The Dragged Surge Motion of Tension-Leg Type Fish Cage System Subjected to Multi-Interactions among Wave and Structures. IEEE Journal of Oceanic Engineering 30(1), 59-78.

Lee, J. F. (1995). On the heave radiation of a rectangular structure. Ocean Engineering 22(1), 19-34.

Mei, C. C. (1983). The Applied Dynamics of Ocean Surface Waves. John Wiley & Sons, Inc., 282-300.

Sarpkaya, T. and M. Isaacson (1981). Mechanics of wave forces on offshore structures. Van Nostrand Reinhold Co., 126-137.

Sollitt, C. K. and R. H. Cross (1972). Wave Transmission through Permeable Breakwaters. Proc. 13th ICCE, 3, 1827-1846.

Tabeshpour, M. R., B. A. Ashtiani, M. S. Seif and A. A. Golafshani (2013). Hydrodynamic damped pitch motion of tension leg platforms. Int. J. MAr. Sci. Eng. 3(2), 91-98.

Tabeshpour, M. R., A. A. Golafshani, B. A. Ashtiani and M. S. Seif (2006). Analytical solution of heave vibration of tension leg platform. J. Hydrology and Hydromechanics 54(3), 280-289,.

Weng, W. K. and C. R. Chou (2007). Analysis of Responses of Floating Dual Pontoon Structure, China Ocean Engineering 20(1), 91-104.

Zhao, X. and C. Hu (2012). Numerical and experimental study on a 2-D floating body under extreme wave conditions. Applied Ocean Research 35, 1-13.